Selective Examination of Heme Protein Azide Ligand-Distal Globin Interactions by Vibrational Circular Dichroism

Richard W. Bormett,[†] Sanford A. Asher,*[,†] Peter J. Larkin,[†] William G. Gustafson,[†] N. Ragunathan,[‡] Teresa B. Freedman,[‡] Laurence A. Nafie,[‡] Sriram Balasubramanian,[§] Steven G. Boxer,[§] Nai-Teng Yu,[∥] Klaus Gersonde,[⊥] Robert W. Noble,[●] Barry A. Springer,[▽] and Stephen G. Sligar[▽]

Contribution from the Department of Chemistry, University of Pittsburgh, Pittsburgh, Pennsylvania 15260, Department of Chemistry, Syracuse University, Syracuse, New York 13244, Department of Chemistry, Stanford University, Stanford, California 94305, School of Chemistry, Georgia Institute of Technology, Atlanta, Georgia 30332, the Hong Kong University of Science and Technology, Hong Kong, Hauptabteilung Medizintechnik, Fraunhofer-Institut für zerstörungsfreie Prüfverfahren, D-6670 St. Ingbert and Fachrichtung Medizintechnik, Universität des Saarlandes, D7650 Homburg/Saar, Germany, Department of Medicine and Biochemistry, State University of New York at Buffalo, Veterans Administration Hospital, Buffalo, New York 14215, and Department of Biochemistry, University of Illinois at Urbana-Champaign, Urbana, Illinois 61801. *Received June 3, 1991*

Abstract: Vibrational circular dichroism (VCD) spectra of the antisymmetric stretch of azide ligated to the heme of a series of evolutionarily diverse and site-directed mutant hemoglobins and myoglobins are anomalously intense and demonstrate an intriguing sensitivity to subtle protein-ligand interactions. The antisymmetric stretch of the azide ligand covalently bound to the low-spin iron shows an anisotropy ratio of -9.5×10^{-4} for sperm whale and horse myoglobin which decreases to -8.0×10^{-4} for human and carp hemoglobin and Chironimus thummi thummi III monomeric hemoglobin. The VCD spectra of these heme-azide complexes depend upon the interactions of the azide ligand with distal heme pocket residues such as the E7 distal histidine and E11 valine. The site-directed mutants of sperm whale (distal histidine substituted Gly E7) and human (distal valine substituted Asn E11) myoglobin have vanishingly small anisotropy ratios ($<-0.5 \times 10^{-4}$), while elephant myoglobin (distal histidine substituted Gln E7) shows an anisotropy ratio of -6.4×10^{-4}. The azide ligand ionically bound to a high-spin iron shows a vanishingly small VCD intensity.

Introduction

The molecular basis of the control mechanism determining ligand affinity in heme proteins remains elusive in spite of the heroic, intensive efforts made over the last century to study the hemoglobin cooperativity mechanism. Numerous specific interactions have been proposed and examined such as strain associated with tension at the proximal (His F8) histidine-iron linkage, specific constraints on the heme geometry through particular orientations of the vinyl groups, and interactions between distal amino acid residues and ligands bound to the heme iron.[1] The difficulty in resolving the importance of these interactions derives from the insensitivity of techniques to these weak interactions.

In this study we demonstrate the use of vibrational circular dichroism (VCD) for studying myoglobin (Mb) and hemoglobin (Hb) interactions with an azide ligand bound to the heme iron.[2] The work here follows the pioneering observation of Marcott and Moscowitz in 1979 of an anomalously large VCD signal for the antisymmetric azide stretch of azidomethemoglobin (HbN_3).[3] We examine this phenomenon for the first time in detail by using evolutionarily diverse and site-directed mutants of Hb and Mb. We correlate the magnitude of the VCD anisotropy ratio with interactions between the azide ligand, the heme iron, and the distal E7 and E11 residues. It appears that VCD may be of incisive utility for studying certain types of ligation of metalloenzymes.

Experimental Section

The sperm whale and horse Mb samples were prepared by dissolving the lyophilized protein (Sigma Chemical Co.) in potassium phosphate (pH 7.1, 0.1 M) buffer. The samples were centrifuged, and the azidometmyoglobin (MbN_3) complex was produced by the addition of a small quantity of a 1 M sodium azide solution. The final protein concentration was ca. 15 mM with an azide concentration of ca. 12 mM.

The preparation of site-directed mutant (Gly E7) sperm whale Mb has been described previously.[4] The mutant sperm whale Mb was purified by chromatography on a column of CM-C50 Sephadex ion exchange resin (Pharmacia Fine Chemicals) which was equilibrated with pH 6.40 phosphate buffer (0.045 M). A pH gradient (pH 6.4-7.0) was used to exchange the protein from the column. The protein was collected, extensively dialyzed against pH 6.40 potassium phosphate buffer (0.045 M), and concentrated using an Amicon ultrafiltration concentrator to ca. 10 mM. The mutant (Gly E7) sperm whale MbN_3 complex was prepared by the addition of a small volume of sodium azide (2.0 M) stock solution to give a final azide concentration of ca. 100 mM.

Reconstituted sperm whale Mb was prepared by the method of Teale[5] using iron deuteroporphyrin (Porphyrin Products). The reconstituted myoglobin was purified on a DEAE Sephadex (Pharmacia Fine Chemicals) column equilibrated with pH 7.1 phosphate buffer (0.05 M). The main protein fraction was collected and concentrated to ca. 10 mM. The concentrations were determined using a molar absorptivity of $\epsilon = 128$ cm^{-1} mM^{-1} for the Soret maximum (393 nm) of the reconstituted aquometmyoglobin.[6] The reconstituted sperm whale MbN_3 complex was prepared by the addition of a small quantity of 1 M sodium azide to yield a heme to azide ratio of 0.9.

* Author to whom correspondence should be sent.
[†] University of Pittsburgh.
[‡] Syracuse University.
[§] Stanford University.
[∥] Georgia Institute of Technology and the Hong Kong University of Science and Technology.
[⊥] Fraunhofer-Institut für zerstörungsfreie Prüfverfahren.
[●] State University of New York at Buffalo.
[▽] University of Illinois at Urbana-Champaign.

(1) Dickerson, R. E.; Geis, I. *Hemoglobin, Structure, Function, Evolution, and Pathology*; Benjamin Cummings Publishing Company Inc.: Menlo Park, CA, 1983.
(2) (a) Asher, S. A.; Larkin, P.; Ragunathan, N.; Freedman, T.; Nafie, L. A.; Springer, B.; Sligar, S.; Noble, R. *Biophys. J.* **1990**, *57*, 50a. (b) Asher, S. A.; Bormett, R. W.; Larkin, P. J.; Gustafson, W. G.; Ragunathan, N.; Freedman, T. B.; Nafie, L. A.; Yu, N.-T.; Gersonde, K.; Noble, R. W.; Springer, B. A.; Sligar, S. G.; Balasubramanian, S.; Boxer, S. G. In *Spectroscopy of Biological Molecules*; Hester, R. E., Girling, R. B., Eds.; Royal Society of Chemistry; Cambridge, England, 1991; pp 139-140.
(3) (a) Marcott, C.; Havel, H. A.; Hedlund, B.; Overend, J.; Moscowitz, A. In *Optical Activity and Chiral Discrimination*; Mason, S. F., Ed.; D. Reidel Publishing Co.: New York, 1979; pp 289-292. (b) Marcott, C. Personal communication, 1990.
(4) Springer, B. A.; Egeberg, K. D.; Sligar, B. A.; Rohlfs, R. J.; Mathews, A. J.; Olson, J. S. *J. Biol. Chem.* **1989**, *264*, 3057-3060.
(5) Teale, F. W. J. *Biochim. Biophys. Acta* **1959**, *35*, 543.
(6) Tamura, M.; Woodrow, G. V.; Yonetani, T. *Biochim. Biophys. Acta* **1973**, *317*, 34.

0002-7863/92/1514-6864$03.00/0

Table I. Anisotropy Ratios of Various Heme Protein Complexes Calculated by Integrating Absorbance and VCD Peak Areas

	MbN_3 and HbN_3 anisotropy ratios $g/10^{-4}$
myoglobins	
native horse	−9.5
native sperm whale	−9.5
deuteroheme-substituted sperm whale (no vinyl groups)	−9.5
mutant sperm whale (Gly E7)	~0.0
Asian elephant (Gln E7)	−6.4
mutant human (Asn E11)	~0.0
hemoglobins	
human without IHP	−8.0
human with IHP	−8.0
Carp without IHP	−8.0
carp with IHP	−8.0
CTT III	−8.0

Asian elephant Mb was purified from skeletal muscle as described by Romero-Herrera et al.[7] Ferric elephant Mb was prepared by oxidation with excess potassium ferricyanide followed by extensive dialysis against 0.01 M (pH 6.6) phosphate buffer adjusted to an ionic strength of 0.1 with potassium chloride. The protein was concentrated to ca. 7 mM in heme, and the elephant MbN_3 complex was formed by the addition of a small quantity of 1 M sodium azide, producing an equimolar heme–azide solution of ca. 6 mM.

Chironomous thummi thummi III monomeric Hb (CTT III Hb) was purified as described elsewhere.[8] CTT III HbN_3 was prepared in a manner similar to that for elephant Mb and concentrated to ca. 7 mM in heme. The ferric mutant human Mb (Asn E11) was purified as described elsewhere[9] and dialyzed and concentrated to ca. 9 mM in a manner similar to that for elephant Mb. The azide complex was prepared by the addition of a small volume of 1 M sodium azide to give a total azide concentration of 10 mM.

A stock solution of human Hb was prepared by dissolving lyophilized human Hb (Sigma Chemical Co.) in deionized, purified water and oxidizing it with excess potassium ferricyanide. The excess potassium ferricyanide was removed by extensive dialysis against purified water. A stock carp Hb solution was prepared as previously described.[10] The frozen stock carp Hb was thawed and centrifuged to remove any precipitate. A Bistris buffer was prepared at a high concentration and added to the stock Hb protein solutions to yield a final buffer concentration of 100 mM Bistris and NaCl at pH 6.0. The final Hb concentration was 10.3 mM in heme. The inositol hexaphosphate (IHP) saturated Hb was prepared by the addition of a small quantity of a concentrated IHP solution to yield a 1 mM excess concentration over that of Hb. This ensured sufficient IHP to saturate the Hb. The azide complexes were prepared by the addition of a small quantity of 1 M sodium azide to produce an equimolar heme and azide solution.

The aqueous protein FTIR and dispersive VCD spectra were acquired at Syracuse University by using a calcium fluoride cell with a ca. 25-μm Teflon spacer. The instrumentation has been described in detail elsewhere.[11] The anisotropy ratios were determined by using the ratio of the integrated VCD and IR peak areas.

Results and Discussion

VCD results from the preferential absorption of left (A_L) or right (A_R) circularly polarized light during a vibrational transition of a chiral molecule.[12] An experimentally determined parameter is the anisotropy ratio, g, where

$$g = \frac{4R}{D} = \frac{\Delta A}{A} = \frac{A_L - A_R}{0.5(A_L + A_R)} = \frac{4Im(\mu \cdot m)}{|\mu|^2} \qquad (1)$$

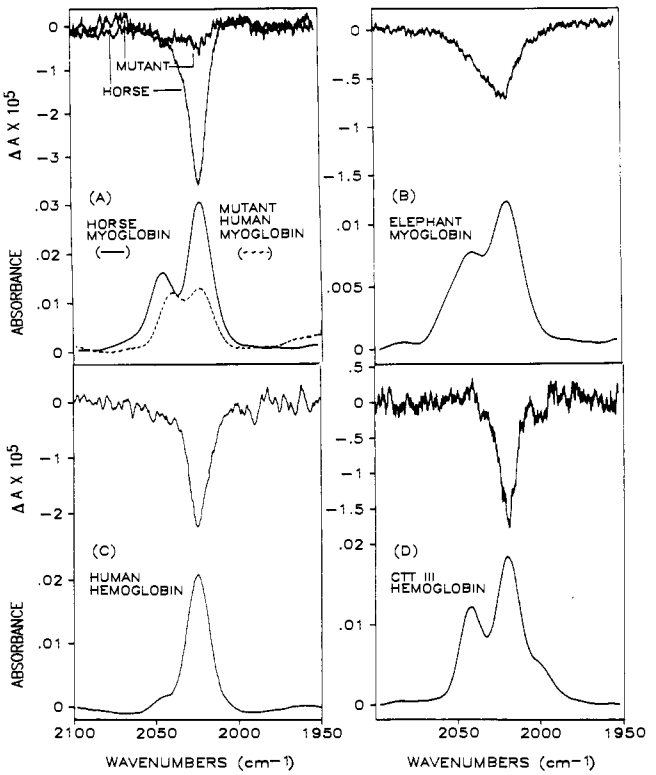

Figure 1. IR absorption (8-cm^{-1} resolution) and VCD (6-cm^{-1} resolution) spectra of the following: (A) 11.5 mM horse MbN_3 and 7.1 mM mutant (Asn E11) human MbN_3 with 2.7 mM unbound N_3^-; (B) 6.0 mM elephant MbN_3; (C) 8.0 mM human HbN_3; (D) 6.0 mM CTT III HbN_3, pH 7 with 0.01 M phosphate buffer adjusted to an ionic strength of 0.7 with KCl. All spectra were measured in a 26-μm CaF_2 cell, and contributions from uncomplexed azide were numerically removed.

μ and m are the transition electric dipole and magnetic dipole moments for the vibrational transition, and R and D are the rotational and dipole strengths, respectively.

The principles underlying VCD are similar to those of electronic circular dichroism (CD). CD is a well-known technique used in studying electronic transitions of chiral molecules; for example, CD measurements of the amide electronic transitions are used to determine protein secondary structure.[13] Analogously, VCD of the amide I band of polypeptides has also been shown to correlate to protein secondary structure.[14] While significant effort has been expended in the examination of VCD phenomena,[12] the technique has not as yet been routinely applied to large molecules.

Figure 1 shows the IR and VCD spectra of azide antisymmetric stretches of several heme protein–azide complexes. Table I lists the measured g values. These g values, which are the largest observed for a localized vibrational mode, are 10-fold smaller than the values (0.02) reported by Marcott et al.[3a] probably because of the less refined instrumentation available at that time.[3b] HbN_3 and MbN_3 show at least two IR bands that result from high- and low-spin-state iron complexes which are in thermal equilibrium.[15] The ~2044-cm^{-1} band derives from the ionically bound high-spin azide, whereas the ~2022-cm^{-1} band derives from the covalently bound low-spin azide;[15] the spin state equilibrium differs between proteins, but usually favors low spin.[16] We have numerically removed the spectral contribution from the small amounts of free azide present.

(7) Romera-Herrera, A. E.; Goodman, M.; Dene, H.; Bartnicki, D. E.; Mizukami, H. *J. Mol. Evol.* **1981**, *17*, 140.
(8) Gersonde, K.; Sick, H.; Wollmer, A.; Buse, G. *Eur. J. Biochem.* **1972**, *25*, 181.
(9) Varadrajan, R.; Lambright, D. G.; Boxer, S. G. *Biochemistry* **1989**, *28*, 3771.
(10) Tan, A. L.; De Young, A.; Noble, R. W. *J. Biol. Chem.* **1973**, *247*, 2493.
(11) Freedman, T. B.; Cianciosi, S. J.; Ragunathan, N.; Baldwin, J. E.; Nafie, L. A. *J. Am. Chem. Soc.* **1991**, *113*, 8298.
(12) Freedman, T. B.; Nafie, L. A. In *Topics in Stereochemistry*; Eliel, E., Wilen, S., Eds.; Wiley: New York, 1987; Vol. 17, pp 113–206.
(13) Woody, R. W. *J. Polym. Sci., Part D: Macromol. Rev.* **1977**, *12*, 181–320. Brahms, S.; Brahms, J. *J. Mol. Biol.* **1980**, *138*, 149–178. Yang, J. T.; Wu, C. H.; Martinez, H. M. *Methods Enzymol.* **1986**, *130*, 208–269. Johnson, W. C., Jr. *Methods Biochem. Anal.* **1985**, *31*, 61–163.
(14) Lal, B. B.; Nafie, L. A. *Biopolymers* **1982**, *21*, 2161–2183. Pancoska, P.; Yasui, S. C.; Keiderling, T. A. *Biochemistry* **1989**, *28*, 5917–5923.
(15) McCoy, S.; Caughey, W. S. *Biochemistry* **1970**, *9*, 2387–2392. Alben, J. O.; Fager, L. Y. *Biochemistry* **1972**, *11*, 842–847.
(16) Asher, S. A.; Larkin, P. J.; Bormett, R. W.; Gustafson, W. G. *Biochemistry* to be submitted for publication.

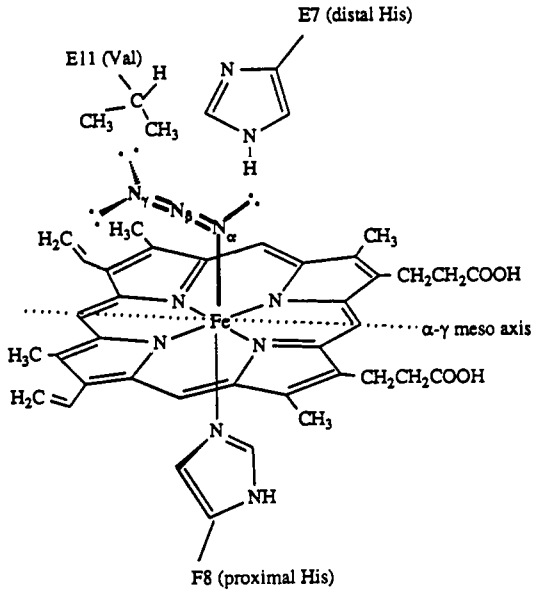

Figure 2. Diagram showing the heme and bound azide ligand interactions with the Val E11 and His E7 in the distal heme pocket. (Heme structure and distal environment is adopted from ref 21.)

Only the low-spin complexes show a VCD signal probably because the ionically bound high-spin-iron–azide ionic bond cannot act as a charge flow conduit into the heme. It is also possible that the high-spin complex could have unfavorable ligand orientation and/or specific distal interactions for VCD to occur. Our new results show that the vinyl groups are uninvolved in the VCD phenomenon since deuteroheme-substituted sperm whale MbN_3 (which contains no vinyl groups) shows the same g value as the native protein (Table I). This contradicts the previous proposal of vinyl group involvement in the VCD phenomenon.[12]

The heme distal pocket is defined by residues at position CD1 (between the C and D helices) and at E7 and E11 (on the E helix). These residues are usually phenylalanine (Phe), histidine (His), and valine (Val), respectively. Only the Phe CD1 is conserved while His E7 and Val E11 are typically present. Negligible VCD differences are seen for proteins with identical heme pockets, such as horse and native sperm whale Mb (Table I). Site-directed mutant myoglobin replacement of His E7 with glycine (Gly) or replacement of Val E11 with asparagine (Asn) results in a near zero g value (Table I) indicating some specific interactions of Val E11 and His E7 with the azide ligand. A further indication of the importance of the E7–azide interaction is the ~35% decreased g value for elephant MbN_3 where glutamine (Gln) replaces His E7.

Human and carp Hb exhibit an ~20% decrease in the g value compared to that of horse Mb. Furthermore, the Hb VCD g value remains unchanged when the protein undergoes the R to T quaternary structural changes induced by inositol hexaphosphate. The g value of the low-spin carp HbN_3 complex remains unchanged even though the protein undergoes a large spin state change in which the low-spin population decreases from 89% to 57%.[17] The unchanged g value indicates that the protein structural alterations that dramatically change the spin state equilibrium do not significantly affect the azide–protein interactions in the low-spin complex that are important for generating VCD. These spin state equilibrium alterations probably result from structural changes on the proximal side of the heme.

C. thummi thummi III (CTT) monomeric Hb has a radically different heme pocket compared to horse Mb.[18] The major conformation of CTT Hb has the heme rotated by 180° about the α–γ meso axis (Figure 2) compared to that of horse Mb.[18,19] However, His E7 and Phe CD1 are conserved, and the E11 residue is isoleucine (Ile E11). CTT HbN_3 shows three bands for the azide antisymmetric stretch, while the VCD spectrum shows two bands. The additional IR and VCD band at 2001 cm^{-1} may result from the α–γ rotoisomer of the heme or the silent point mutation,[19] 57E6 (Thr/Ile), in the heme cavity.

The change in the distal heme environment of CTT III HbN_3 results in a 20% decreased g value compared to that for horse MbN_3. This decreased VCD intensity is similar to that for human and carp Hb which also have less constrained heme pockets compared to Mb. The equivalent g values for the 2001- and 2020-cm^{-1} bands suggest that only specific protein–ligand interactions are important in determining the magnitude of g, and that the heme–protein interactions that cause the 20-cm^{-1} decrease in the azide antisymmetric stretch do not significantly alter the g value.

The distal Gln E7 of elephant Mb has two terminal amine hydrogens sufficiently close to hydrogen bond to the azide. In addition, the O_2, CO, and CN complexes of elephant Mb have Phe CD4 within van der Waals' distance of the ligands.[20] It is believed that Gln E7 shifts toward heme pyrrole IV to accommodate Phe CD4.[20] This would produce a more constrained, hydrophobic distal environment which may be responsible for the increased IR and VCD peak widths and the presence of an additional, presumably ionically bound high-spin, IR band (unresolved at 8-cm^{-1} resolution) at 2054 cm^{-1} for the elephant MbN_3. The asymmetry of the VCD band also suggests a contribution from an unresolved covalently bound azide band underlying the 2041-cm^{-1} ionically bound azide band. The presence of an additional covalent band at 2041 cm^{-1} and an additional ionic band at 2054 cm^{-1} suggests that the azide ligand binds in two distinct conformations within the heme pocket of elephant Mb.

The 2019-cm^{-1} elephant MbN_3 g value is 35% less than that of proteins with a distal histidine (E7). This reduced g value probably results from altered hydrogen bonding of the ligand with the Gln E7 compared to His E7. Differences in the sequences of elephant Mb and horse Mb other than Gln E7 substitution are distant from the heme pocket and should not affect ligand binding.

Any attempt to understand the origin of the heme–azide VCD spectra must simultaneously take into account the extraordinarily large g value and its negative sign. For a negative g value, the electric and magnetic dipole transition moments must orient in roughly opposite directions such that their scalar vector projection on one another is negative, and the magnetic dipole transition moment must be unusually large in relation to the accompanying electric dipole transition moment (eq 1).

The most likely source of the large circulating electron current for the magnetic dipole transition moment is the heme ring (Figure 2) with its large number of π-electrons (approximately 20). The heme–azide moiety and the surrounding protein pocket represent a molecular system that is too complex to model using molecular orbital calculations of VCD intensity. Further, existing models of VCD intensity do not yet provide a sound enough basis for a reliable interpretation of the VCD spectra at the level of detail provided by the experimental data.

In the most general terms, we have here a set of VCD spectra originating from a *lone* azide oscillator perturbed by the chiral environment of the heme pocket. Models of VCD based on the coupling of *two or more* roughly equivalent chirally oriented oscillators can thus be ruled out for this system. The observed g value of the VCD near 10^{-3} requires that the lone azide oscillator generate a large magnetic dipole transition moment, presumably by long-range electron flow through (1) the coupling of electron current to the nuclear momenta of the azide ligand, (2) a polarizability mechanism, (3) vibronic coupling, or some combination of these sources.

(17) Noble, R. W.; DeYoung, A.; Vitale, S.; Morante, S.; Cerdonio, M. *Eur. J. Biochem.* **1987**, *168*, 563–567.
(18) Steigemann, W.; Weber, E. *J. Mol. Biol.* **1979**, *127*, 309–338. La Mar, G. N.; Overkamp, M.; Sick, H.; Gersonde, K. *Biochemistry* **1978**, *17*, 352–361. La Mar, G. N.; Smith, K. M.; Gersonde, K.; Sick, H.; Overkamp, M. *J. Biol. Chem.* **1980**, *255*, 66–70.
(19) La Mar, G. N.; Anderson, R. R.; Chacko, V. P.; Gersonde, K. *Eur. J. Biochem.* **1983**, *136*, 161–166.
(20) Yu, L. P.; La Mar, G. N. *Biochemistry* **1990**, *29*, 2578–2585.
(21) Stryer, L.; Kendrew, L. C.; Watson, H. C. *J. Mol. Biol.* **1964**, *8*, 96–104.

Conclusions

In this study we demonstrate the utility of VCD as a new biophysical technique for studying ligand binding in metalloenzymes. Because of the sensitivity of VCD to energetically small interactions between the azide ligand and the E7 and E11 distal residues, which provide a chiral environment for the prochiral azide ligand, VCD studies have the potential to provide a new view of the subtle molecular interactions that influence ligand binding. Although other possibilities cannot be ruled out, our analysis strongly suggests that the source of the enhanced magnetic dipole strength is vibrationally induced current in the delocalized electrons of the heme plane. In the context of this interpretation, the results of these experiments reveal the presence of a long-range electronic communication between the heme, its ligands, and the distal protein residues to which VCD is sensitive.

Acknowledgment. We thank Dr. Curt Marcott for help in the early stages of this work. We gratefully acknowledge support for this work from NIH Grants IR01GM30741-09 (to S.A.A.), GM23567 (to L.A.N. and T.B.F.), 5P01-HL40453 (to R.W.N.), GM33775 and GM31756 (to S.G.S.), GM18894 (to N.-T.Y.), and GM27738 (to S.G.B.). We also acknowledge support for this work by the Fond der Chemischen Industrie and the Medizinische Biophysik e.V. (to K.G.).

Solid-State NMR Studies of the Molecular Motion in the Kaolinite:DMSO Intercalate

Melinda J. Duer,* João Rocha, and Jacek Klinowski

Contribution from the Department of Chemistry, University of Cambridge, Lensfield Road, Cambridge CB2 1EW, U.K. *Received July 15, 1991*

Abstract: The structure and motion of the guest molecule in the interlayer space of the kaolinite:DMSO intercalation compound have been studied by ^2H NMR spectroscopy of static samples, ^{13}C, ^{27}Al, and ^{29}Si high-resolution solid-state NMR spectroscopies, variable-temperature powder X-ray diffraction, and Fourier transform infrared spectroscopy. The guest DMSO molecules are hydrogen-bonded via the oxygen atom to the kaolinite hydroxyls which face the interlayer space, and there is a degree of interaction between the sulfur atom of the DMSO molecule and the siliceous matrix of kaolinite. There are two independent sites for the DMSO methyl groups with effective ^2H quadrupole coupling constants of 59 and 67 kHz, and the population of at least one site is in motion. The difference in these couplings probably reflects different geometries of the methyl groups in the two sites, caused by their partial "keying" into the siliceous matrix. Three motional models produce simulations which are in acceptable agreement with the experimental spectra. One fit is consistent with the keying of one methyl group of a DMSO molecule into the kaolinite layer and raises an interesting point concerning the packing of the DMSO molecules in the interlayer spacing. Above ca. 339 K further exchange processes must be taken into account in ^2H NMR line shape simulations and may trigger structural transformations of the intercalate.

Introduction

Intercalation of clays such as kaolinite has led to the development of materials with novel rheological, surface, and structural properties which have found applications in the paper industry, in polymer composites, as matrices for slow release of trapped molecules, and as soil conditioners.[1-3] Kaolinite is a dioctahedral (1:1) layered aluminosilicate with the chemical formula $Si_2O_5(OH)_4Al_2$. The kaolinite layer can be regarded as the result of a fusion of the $(Si_2O_5)_n^{2-}$ layer and the $Al(OH)_3$ (gibbsite) layer (Figure 1). Wada[4] has found that inorganic salts such as potassium acetate penetrate the interlayer space of kaolinite. Small and highly polar molecules such as dimethyl sulfoxide (DMSO) can also be directly intercalated into kaolinite. These results have triggered a considerable amount of research into the formation and structure of the interlayer complexes of kaolinite.

Some attention has been given to the structure of the kaolinite:DMSO intercalate,[5-14] and several solid-state NMR studies have appeared.[10-14] However, there has been no study of the molecular motion of DMSO in the interlayer space, which may be an important factor in determining the structure and properties of the intercalation compound. Upon intercalation, the (001) kaolinite lattice spacing increases from 7.17 to 11.26 Å, and this increase in spacing has been used to differentiate between kaolinite and serpentite group minerals. Unfortunately, suitable single crystals of kaolinite are not available. Further, because of peak overlap the Rietveld method[15] is of limited value for structures with large, low-symmetry unit cells. However, infrared (IR) and NMR studies can supplement the structural information available from X-ray diffraction (XRD).[12] The two published attempts to solve the kaolinite:DMSO intercalate structure used quasi-single-crystal methods in tandem with IR and solid-state NMR

(1) Theng, B. K. G. In *The Chemistry of Clay-Organic Reactions*; Adam-Hilger: London, 1974.
(2) Theng, B. K. G. *Clays Clay Miner.* **1982**, *30*, 1.
(3) Lagaly, G. *Philos. Trans. R. Soc. London* **1984**, *A311*, 315.
(4) Wada, K. *Am. Mineral.* **1961**, *46*, 78.
(5) Weiss, A.; Thielepape, W.; Orth, H. In *Proceedings of the International Clay Conference*, Jerusalem; Heller, L., Weiss, A., Eds.; Israel Program for Scientific Translations: Jerusalem, 1966; Vol. 1, p 277.
(6) Olejnik, S.; Aylmore, L. A. G.; Postner, A. M.; Quirk, J. P. *J. Phys. Chem.* **1968**, *72*, 241.
(7) Sanchez Camazano, M.; Gonzalez Garcia, G. *An. Edafol. Agrobiol.* **1970**, *29*, 651.
(8) Jacobs, H.; Sterckx, M. In *Proceedings of the Reunion Hispano-Belge Miner. Arg.*, Madrid; Serratosa, J. M., Ed.; CSIC: Madrid, 1970; p 154.
(9) Adams, J. M.; Waltl, G. *Clays Clay Miner.* **1980**, *28*, 173.
(10) Thompson, J. G. *Clays Clay Miner.* **1985**, *33*, 173.
(11) Thompson, J. G.; Cuff, C. *Clays Clay Miner.* **1985**, *33*, 490.
(12) Raupach, M.; Barron, P. F.; Thompson, J. G. *Clays Clay Miner.* **1987**, *35*, 208.
(13) Duer, M. J.; Klinowski, J.; Rocha, J. The Study of Intercalated Molecules Using One- and Two-Dimensional Solid-State NMR. Ampère Conference, Stuttgart, September 1990.
(14) Rocha, J.; Kolodziejski, W.; Klinowski, J. *Chem. Phys. Lett.* **1991**, *176*, 395.
(15) Rietveld, H. M. *J. Appl. Crystallogr.* **1969**, *30*, 65.

0002-7863/92/1514-6867$03.00/0